Mechanisms of Second Harmonic Generation Efficiency Relaxation in Poled Guest/Host Polymers

Stephan Schüssler,‡ Ranko Richert,*,† and Heinz Bässler‡

Fachbereich Physikalische Chemie und Zentrum für Materialwissenschaften, Philipps-Universität Marburg, 35032 Marburg, Germany, and Max-Planck-Institut für Polymerforschung, Ackermannweg 10, 55128 Mainz, Germany

Received September 22, 1994; Revised Manuscript Received December 29, 1994[⊗]

ABSTRACT: We have investigated the second harmonic generation (SHG) signals of a guest/host system based on 4−(dimethylamino)-4′-nitrostilbene dissolved at 1 wt % in poly(isobutyl methacrylate) and poled in a sandwich configuration of ITO electrodes. By blocking the injection from the ITO surfaces with SiO coatings, a significant impact of charge carriers on the SHG decay pattern can be excluded. Using chloroform as a solvent, an additional contribution to the SHG decay kinetics is observed which is also active in the presence of the external electric poling field. Separating this effect from the pure orientational relaxation of the dopants leads to a highly improved reproducibility. Due to its weak temperature dependence, we tentatively ascribe this solvent-specific effect to the diffusion of dipolar impurities which may affect the local field factors and hyperpolarizability tensors. The resulting corrected SHG time constants related to the pure orientational relaxation still appear to be strongly decoupled from the α-process of the matrix as inferred from dielectric relaxation data of the bulk polymer. This basic discrepancy between SHG decay and α-process is found not to depend on film preparation, sample conductivity, sample geometry, and residual solvent content.

Introduction

Since the first report of electric field poling of doped polymer films[1] to break the inherent centrosymmetry and the demonstration that by such a process large second-order nonlinear optical (NLO) coefficients are obtained, there has been a great effort to employ this technique for polymer science and commercial application.[2−6] The motivation for using polymers with NLO properties is related to the production of the inexpensive and custom-tailored materials for optical data storage and electrooptical devices as well as alternatives for inorganic crystals used in second harmonic generation (SHG), the conversion of light of the frequency ω to twice the frequency, i.e., 2ω.[7,8]

The inevitable tendency for thermal randomization of such a noncentrosymmetrically aligned ensemble of dopants after the removal of the dc poling field has been the subject of intense research. The decay of the SHG intensity is related to the decay of the second-order macroscopic susceptibility $\chi^{(2)}$.[4,9] Hence, particular interest has been laid on employing SHG relaxation measurements as an in situ method to either investigate the long-term stability of dopant alignments for technical purposes or to use the reorientation of a dopant as a probe of the dynamic properties of the surrounding matrix cages. However, the relaxation pattern can be affected by various parameters such as the temperature, the molecular structure and free volume of the system, and as the presence of charges and dipoles within the material. Thus, SHG relaxation studies offer a powerful tool to gain insight into the basic local processes causing the orientational randomization of dopant molecules.

Following the discussion in the literature, the temperature dependence of the rate of these decays and the shape of the relaxation pattern itself often differ significantly even when working with quite similar materials. One important question in this context concerns the extent of coupling of the dopant's movement to the α-relaxation of the matrix. Various different approaches involving time-resolved optical spectroscopy,[10] transient grating experiments[11−13] as well as dielectric measurements[14,15] and thermally stimulated discharge experiments (TSD)[16] have been applied to characterize the dynamics of guest molecules in polymer host materials. The interest in a more complete understanding of the SHG decay experiment stems also from the observed quantity being highly selective to the orientation of the chromophores.

The main purpose of this work is to identify experimental factors which may affect the results and to find ways to separate them from intrinsic material properties, thereby extending our previous studies.[17] In the following we will report on SHG measurements using electrode-poled films of 4-(dimethylamino)-4′-nitrostilbene (DANS) dissolved at 1 wt % in poly(isobutyl methacrylate) (PIBMA). The influence of electrical conductivity and different sample setup on the relaxation pattern is analyzed. A deeper insight into the randomization dynamics after switching off the electric field is achieved by quantitatively taking into account a significant SHG decay while the field is still applied. Highly reproducible relaxation data were collected within an expanded temperature regime encompassing the glass transition T_G, the fits being based on a Gaussian distribution of energy barriers for the reorientation process. This set of data is compared to dielectric measurements of the pure matrix material. Special emphasis is laid on the influence of changing the solvent used for film preparation.

Theoretical Aspects

Second-order NLO properties, including SHG, are usually expressed in terms of the second-order susceptibility $\chi^{(2)}(-2\omega;\omega,\omega)$ tensor in the polarization relationship P for the bulk material[4]

$$P = \chi^{(1)}E(\omega) + \chi^{(2)}E(\omega)E(\omega) + \chi^{(3)}E(\omega)E(\omega)E(\omega) + \ldots \quad (1)$$

According to the dielectric approximation[4] these $\chi^{(n)}$ tensors measure the macroscopic compliance of the

† Max-Planck-Institut für Polymerforschung.
‡ Philipps-Universität Marburg.
⊗ Abstract published in *Advance ACS Abstracts,* March 1, 1995.

0024-9297/95/2228-2429$09.00/0

electrons. Since $\chi^{(2)}$ is proportional to the square of the field strength of the optical field $E(\omega)$, SHG requires a noncentrosymmetric medium. Hence in polymer guest/host systems the dopants have to be poled by means of a strong electric dc field. Making use of the so-called free-gas approximation,[4] the relevant tensor elements for the macroscopic second-order susceptibility $\chi^{(2)}$ are given by

$$\chi^{(2)}_{333} = Nf_3^2(\omega)f_3(2\omega)\beta_{zzz} \langle \cos^3 \Theta \rangle \quad (2)$$

$$\chi^{(2)}_{311} = Nf_1(\omega)f_3(\omega)f_3(2\omega)\beta_{zzz}(\langle \cos \Theta \rangle - \langle \cos^3 \Theta \rangle) \quad (3)$$

where N is the number of NLO-active molecules per unit volume and $f_i(\nu)$ are dimensionless field factors which are associated with the appropriate macroscopic coordinates (1,2,3) and the optical frequency components. β_{zzz} represents the relevant tensor element of the molecular hyperpolarizability along the dipole axiz z, and Θ measures the angle between the z and 3-direction (being the macroscopic direction of the poling field). Assuming a p-polarized fundamental beam with the electric field $E(\omega)$ and the 1−3-plane as the plane of incidence, the NLO polarization at 2ω is found to be proportional to $\chi^{(2)}_{333}$ and $\chi^{(2)}_{311}$ and thus proportional to the averaged chromophore orientation expressed by $\langle \cos \Theta \rangle$. A further relationship shows that the square root of the SHG intensity is proportional to the NLO polarization at 2ω and therefore strongly related to the dopant orientation. More information concerning these theoretical aspects has been given recently[17] and is available in much more detail elsewhere.[4,9,18]

Experimental Section

1. Sample Preparation. PIBMA of high molecular weight (Elvacite 2045, DuPont; M_w = 193 000, M_n = 120 000; vacuum dried for 6 days at 120 °C to remove possible impurities of low molecular weight) and appropriate amounts of DANS (Kodak) were dissolved in HPLC-grade chloroform (Aldrich) or toluene (Merck) to form solutions of 1 wt % chromophore concentration. The films made from toluene solutions were dried at 50 °C for about 30 min and backed at 75 °C under vacuum for at least 6 days before the sandwich setup was assembled. Films of 25 μm thickness were obtained between two indium tin oxide (ITO, Baltracon 417, Balzers) coated glasses using polyimide spacer sheets (Kapton, DuPont). The exact procedure and a detailed description of the sample architecture have been stated elsewhere.[17] The capacitance of the sandwich cells was about 100 pF.

The optical homogeneity, i.e., absence of aggregation, was checked with a microscope using crossed polarizers. Being aware of the insufficiency of such a test, the actual claim of homogeneity stems from the relaxation data being DANS concentration invariant and highly reproducible.[17] In order to avoid interactions among chromophores and laser-induced heating effects, we limited the experimental conditions to below 1 wt % DANS and ≥300 μm laser spot, respectively. This in turn restricted our usable minimum film thickness to ~20 μm for obtaining sufficiently strong SHG signals. The presently used thickness of 25 μm calls for quantifying the residual solvent content, which by elemental analysis revealed ≈0.8 wt % chlorine for the present preparation and drying technique. Monitoring the solvent removal throughout the drying process by means of UV/vis spectroscopy (Perkin-Elmer Lamda 9) resulted in stationary absorption spectra after 2 days, so that the evolution within the remaining 4 days of drying was inaccessible with this technique.

2. Poling and Thermal Erase. Guided by our previous success concerning reproducibility of SHG data, the following procedure for sample conditioning was applied: Prior to each measurement, the sample was held at 170 °C for 1 h to erase the thermal history and then quenched to 120 °C within 50 s by an air stream. After letting the sample equilibrate for 15 min, a poling field of either 0.14 or 0.10 MV/cm was applied for 5 min in order to saturate the alignment. Control of the poling process was established by in situ monitoring of the SHG signal as well as the cell current. This procedure was followed by quenching to the desired temperature. Simulation of this thermal treatment in a differential scanning calorimetry (DSC) experiment after a thermal erase step yielded $T_G \approx 63$ °C. The DSC scan was performed at a cooling mixture rate of 10 K/min in order to match the rates realized in the SHG experiment.

3. Experiment Setup for the SHG Measurement. The SHG experimental setup involved a 76 MHz mode-locked Nd-YAG laser operated at 1064 nm (~40 nJ/pulse, 250 ps pulse width). The detection of the light at 2ω = 532 nm was done via online normalization using a quartz reference in a second detection channel. Signal processing was established by lock-in techniques. Particularities concerning the relevant experimental factors to be considered have been outlined in detail elsewhere.[17] All results in this paper are presented with the signal-to-noise ratio as originally acquired.

4. Dielectric Measurement. In order to quantify the mean relaxation time in the range of present interest, the frequency-domain response and impedance analysis were employed in the range 10^{-3}−10^7 Hz. To cover this scale two different systems were used: a frequency-response analyzer (Solartron-Schlumberger FRA-1260, 10^{-3}−10^6 Hz) equipped with a Chelsea dielectric interface and an impedance analyzer (HP-4192A, 10^2−10^7 Hz). The sample temperature was adjusted by a temperature controller (Quatro, Novocontrol) using a heated N_2 gas stream and measured independently with a PT-100 sensor.

Following common practice, we fit the symmetrically broadened dielectric loss data $\epsilon''(\omega)$ to the empirical Havriliak−Negami function $\epsilon^*(\omega) = \epsilon'(\omega) - i\,\epsilon''(\omega) = \epsilon_\infty + \Delta\epsilon[1 + (i\omega\tau)^\alpha]^{-\gamma}$, which coincides well with the data in the vicinity of the peak of $\epsilon''(\omega)$. For the present purpose the frequency ω_m, defined by the peak position of $\epsilon''(\omega)$, is employed to designate a characteristic dielectric relaxation time of the α-process in PIBMA. This choice corresponds roughly to the mean relaxation rate $\langle r \rangle$ obtained from time-domain decay data.

Results and Discussion

1. Sample Conductivity. In a recent discussion regarding the conductivity of ITO sandwich poled guest/host polymers using poly(ethyl methacrylate) (PEMA), we concluded that charge injection effects from the electrodes are an important factor.[17] To gain further insight into these phenomena, layers of silicon monoxide (SiO, Balzers) of varying thickness were evaporated onto the anodes for the present study. Introducing SiO blocking coatings in the sandwich cells did not affect the characteristic optical absorption behavior of the sample, but it reduces the cell conductivity by a factor of ≈20 as demonstrated in Figure 1. A further reduction of conductivity could not be acheived by increasing the thickness of the SiO layer. In the course of these conductivity experiments we have also investigated the effect of varying the applied voltage from 0.1 to 0.14 MV/cm. Additionally, the behavior of the undoped matrix as well as the influence of toluene instead of chloroform as a solvent for casting the films has been investigated. All current results as summarized in Figure 2 turned out to be unaffected by irradiation of the sample with the fundamental beam of 1064 nm. Since no difference between the pure matrix and the weakly doped guest/host system has been found, we conclude that in case of these low concentrated materials the conductivity must be an inherent property of the matrix material, most probably due to ionic impurities.

2. SHG Signal Decay with Applied Field. During the poling process of samples cast from chloroform

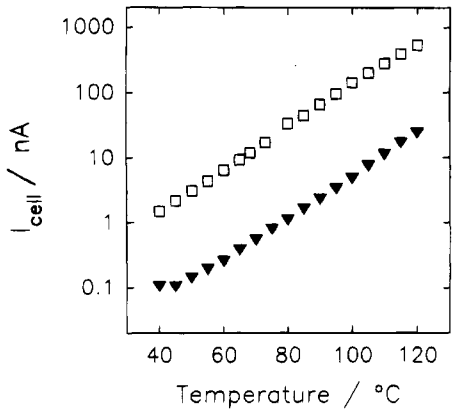

Figure 1. Temperature-invariant reduction of the cell current of a 25 μm PIBMA/DANS film by coating the anode with SiO (filled triangles). The upper curve (open squares) refers to a sample with an uncoated ITO anode.

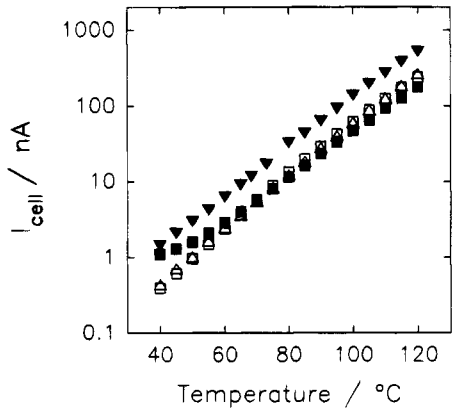

Figure 2. Temperature dependence of the cell current of 25 μm PIBMA films (doped with 1 wt % DANS) under various experimental conditions: filled triangles, uncoated anode, 0.14 MV/cm poling field; open triangles, uncoated anode, 0.10 MV/cm poling field; open squares, uncoated anode, pure matrix material, 0.10 MV/cm poling field; filled squares, uncoated anode, 0.10 MV/cm poling field, film cast from toluene solution instead of chloroform.

solutions, a steady decrease of the intensity at 2ω by up to 80% of the initial value was observed with the field still applied. Common features of this unexpected effect are the time scale of this process of up to several hours and the complete reversibility provided that a thermal erase cycle preceded each experiment. Irreversible effects were occasionally detected when using either fresh samples or samples which had not been used for several days. An explanation for these features cannot be given at present but similar effects have been observed in almost every sample of poly(alkyl methacrylates). A representative decay of the SHG signal with the field applied is depicted in Figure 3. Based on the extent of this effect and its impact on the apparent relaxation process without field, we have started intense efforts to characterize this phenomenon in more detail for the films cast from chloroform solution.

The most simple description of the above decay is an exponential with time constant τ combined with an offset I_∞:

$$I = [(I_0 - I_\infty) \exp(-t/\tau)] + I_\infty \qquad (4)$$

Note that all intensities are related to the square root of the normalized SHG signal, i.e., $I(t) = [I_{SHG}(t)/I_{SHG}(0)]^{1/2}$. The slope m of $I(t)$ at $t = 0$ leads to an

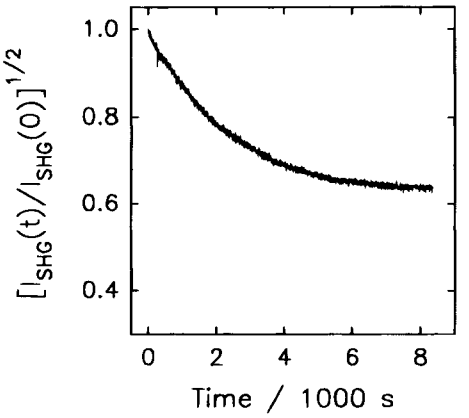

Figure 3. Typical SHG signal decay for a PIBMA sample (cast from a chloroform solution) doped with 1 wt % DANS. The trace is recorded at $T = 45$ °C with the poling field of 0.14 MV/cm being applied during data acquisition.

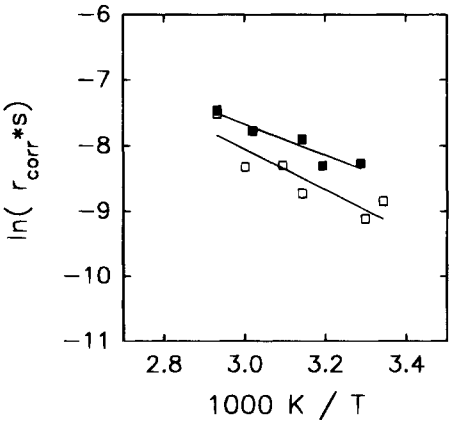

Figure 4. Arrhenius plot of the characteristic times of isothermal SHG decays with applied field. The data refer to a PIBMA sample doped with 1 wt % DANS using an uncoated anode and poling fields of 0.14 (filled squares) and 0.10 MV/cm (open squares).

Table 1. Activation Energies for the SHG Decay as a Function of Electrode Coating and Poling Field

PIBMA sample	poling field (MV/cm)	E_{act} (kJ/mol)	E_{act} (eV)
uncoated anode	0.10	25.9	0.27
uncoated anode	0.14	19.7	0.20
SiO-coated anode	0.10	14.3	0.15
SiO-coated anode	0.14	3.3	0.03

expression for $1/\tau$:

$$\frac{1}{\tau} = \frac{m}{1 - I_\infty} = r_{corr} \qquad (5)$$

Therefore, the saturation level I_∞ has to be determined as accurately as possible. Decay curves under an applied field were recorded in the range 25 °C $\leq T \leq$ 68 °C, analyzed according to eqs 4 and 5, and evaluated in terms of an activation energy by linear regression in an Arrhenius plot. The results are compiled in Table 1 and depicted in Figures 4 and 5.

At elevated temperatures ($T \gg T_G$) the time scale of the decay under field becomes much longer compared to the pattern after switching off the field. Figure 6 presents the result of such an experiment at $T = 90$ °C (T_G + 27 K) where the poling field had been switched off for a certain period of time followed by repoling.

The equivalent behavior below T_G is addressed in Figure 7, which shows data of two measurements at T_G

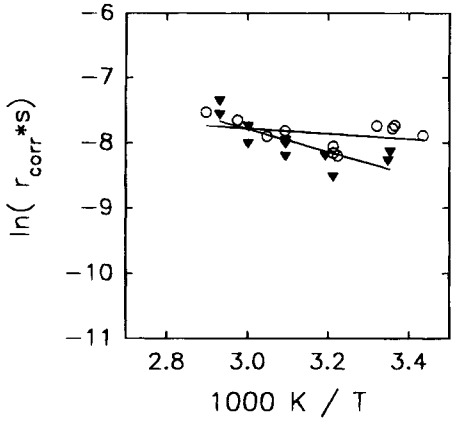

Figure 5. Arrhenius plot of the characteristic time of an isothermal SHG decay with applied field. The data refer to a PIBMA sample doped with 1 wt % DANS using a SiO-coated anode and poling fields of 0.14 (open circles) and 0.10 MV/cm (filled triangles).

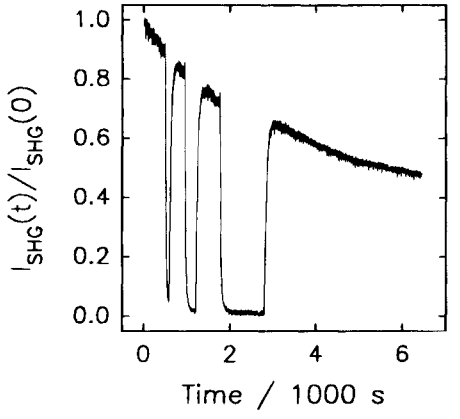

Figure 6. Normalized SHG signal decay for a 1 wt % DANS/PIBMA system at T = 90 °C (T_G + 27 K). The poling field has been switched off for three periods of varying length. The slow decay under field proceeds independent of the presence of an external field.

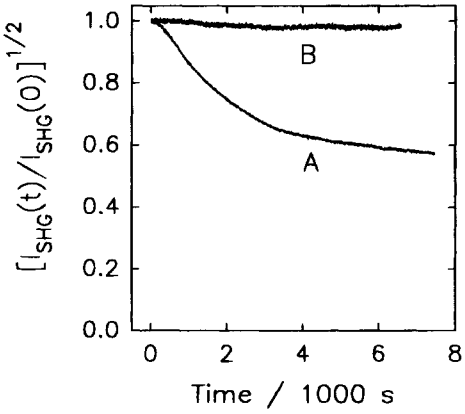

Figure 7. Traces of normalized SHG relaxation in a PIBMA sample doped with 1 wt % DANS at T = 18 °C (T_G − 45 K). Trace A refers to directly switching off the field after having reached a maximum in the signal intensity by poling. Curve B refers to removing the field after a 2:20 h delay at T = 18 °C and 0.14 MV/cm poling field.

− 45 K and carried out under otherwise identical experimental conditions using the same sample as for the 90 °C case. Trace A corresponds to the SHG signal recorded directly after alignment by poling and implies a comparatively fast relaxation of the dopants on a time scale of several hours. In contrast, an almost constant SHG signal level is obtained (trace B in Figure 7) when the poling voltage is maintained for 2:20 h at these low temperatures before switching off the field and recording the subsequent SHG signal. This striking difference between SHG decay under an electric field and that following the removal of the field implies that one tends to interpret the faster process as orientational relaxation of the guest molecules if these two effects are not separated properly.

Even when using the above simplified data analysis, some important features are obvious regarding the thermal behavior of the SHG signal decay with applied field (cf. Figures 4 and 5):

(i) The SHG decay with applied field is only weakly thermally activated with barriers between 3 and 26 kJ/mol, depending on the poling field and electrode coating (see Table 1).

(ii) The absolute rates of the process appear to be insensitive to the various experimental conditions. Despite a reduction of the cell current by more than one order of magnitude, no severe influence on the overall decay is visible.

The most important aspect in this context is the fact that the activation energies for the SHG decay with applied field are far too small to be interpreted in terms of intrinsic polymer motions for this class of matrix materials.[19-22] A qualitative explanation for this phenomenon can be offered when considering the influence of dipolar components or free changes on $\chi^{(2)}$. Elemental analysis of solvent residues in the samples cast from chloroform solutions yielded almost 1% by weight of chlorine, corresponding to about five chloroform molecules per one NLO chromophore. Furthermore, comparing the possible charge density of 10^{10-15} cm^{-3} (estimated assuming a typical current in the nA regime, mobilities of about 10^{-4} cm^2/V s or alternatively via the cell capacitance) with the chromophore density estimated to be 5 × 10^{19} DANS/cm^3 (which is in good agreement with results from Guan[23]) implies that the concentration of free charges is too small to gain any significant impact on the dopants. This assumption is also underlined by the coincidence of experimental decay results for samples with and without blocking electrodes.

Our present picture for rationalizing the SHG relaxation process in the presence of the poling field is as follows. Mainly residual chloroform molecules (μ = 1.01 D[24]) and additional small dipolar impurities (e.g., water) might gradually accumulate around already aligned chromophores by diffusion. Such a process might proceed with low thermal activation, weak field dependence, and independent of an anode coating. It also complies fully with the reversibility being correlated with our thermal erase procedure. Additional evidence stems from the absence of these effects when the less polar toluene instead of chloroform is used. This influence of chloroform is particularly important since most of the published work concerning poled polymers has been done using films cast from chloroform solutions. A further indication for the contribution of only very few solvent molecules to this effect might be the fact that UV/vis spectra of the film taken before and after a thermal erase step did not differ at all.

It remains to be clarified how polar molecules which are free to diffuse within the matrix have a feedback on the SHG efficiency of the sample. First, it is plausible that the chloroform molecules will tend to solvate the DANS selectively because the host polymer is almost nonpolar. We assume that such a shielding

might both seriously weaken the poling field felt by a given chromophore and strongly affect its hyperpolarizability and the local field factors (cf. eqs 2 and 3). These field factors relate the externally applied (optical) fields $E(\omega_i)$ to the corresponding fields $e(\omega_i)$ actually felt by a molecule in the material as a result of charges present on neighboring molecules and any orientational polarization that might occur on adjacent molecules in reaction to the charge distribution on the molecule of interest. Various approaches have been established to calculate these field factors, all being more or less based on comparatively crude simplifications, especially with regard to the geometry of the local environment; i.e., usually uniform polarization of the vicinity is considered. Dynamic and anisotropic effects like those discussed presently are certainly not accounted for. Local field factors are often estimated from the Lorentz expression[4,15]

$$f(\omega) = \frac{\epsilon(\omega) + 2}{3} \tag{6a}$$

or in a more sophisticated approach via the Onsager expression[7]

$$f(\omega) = \frac{(\epsilon_\infty + 2)\epsilon(\omega)}{\epsilon_\infty + 2\epsilon(\omega)} \tag{6b}$$

The validity of eqs 6a and 6b is restricted to spherical symmetries and to a continuum approximation of the dielectric surrounding the dye molecule. Thus it is important to note that even a strong decrease of the SHG intensity is not necessarily associated with a change of $\langle\cos\Theta\rangle$. However, the average orientation quantified by $\langle\cos\Theta\rangle$ might also be affected due to changes in the local poling field as a consequence of molecular inhomogeneities.

According to the literature, the SHG stability of aligned systems has usually been determined only after removing the applied field and assuming that the decrease of the SHG signal is solely related to a change of the dopant averaged orientation. Our novel results alter the interpretation of SHG relaxation patterns since a signal decay in the case of a constant poling field should not relate to orientational randomization of the chromophores. Above T_G the relaxation time scale is dominated by the decay without field as seen in Figure 6. However, below T_G as in Figure 7 there is a significant risk of misinterpreting the decay data, because the time scale of dopant reorientation (trace B) is much longer than the apparent decay time (trace A). Relating trace B of Figure 7 to changes of $\langle\cos\Theta\rangle$ instead of trace A is more sensible in light of the temperature being 45 K below T_G, i.e., close to the Vogel temperature T_0, where motional freedoms are believed to be completely frozen.[25] Effects due to physical aging at such low temperatures on a time scale of 2–3 h are unlikely to occur and can only affect the SHG decay after removing the field, but should not influence the SHG intensity while poling. Aging experiments on a similar time scale using PEMA as a matrix material for SHG studies have also ruled out any significant contribution of aging in this case.[17]

The distinct SHG decay processes with and without field become comparable in time scale at a temperature $T \approx 50$ °C. Figure 8 presents a set of normalized SHG data obtained at this temperature (T_G − 13 K) recorded directly without a preceding signal loss while poling, i.e.,

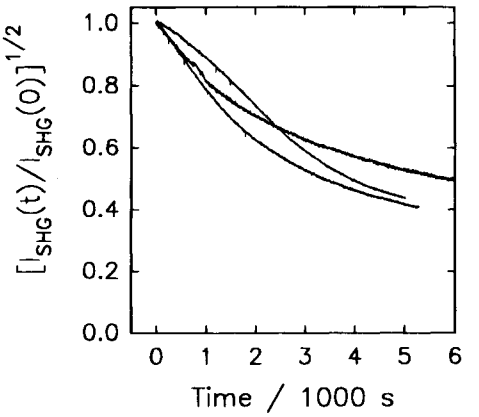

Figure 8. Set of normalized SHG decays of a PIBMA sample (from chloroform solution) doped with 1 wt % DANS at T = 50 °C (T_G − 13 K). The SHG decay due to pure dopant reorientation is superimposed by shielding effects of poor reproducibility.

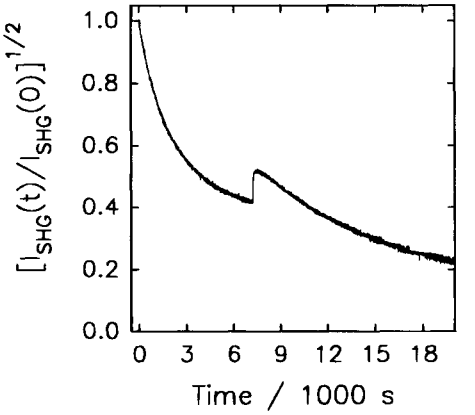

Figure 9. Normalized time dependence of the SHG signal in a PIBMA sample doped with 1 wt % DANS at T = 60 °C (T_G − 3 K). The poling voltage has been switched off at t = 7500 s, which results in changes of the decay pattern.

in the usual manner. Referring to our explanations of the decay under field, the bad reproducibility in this case stems from the competition of the poorly defined decay by chloroform shielding and the "real" orientational effect which proceed simultaneously. For this experiment a numerical analysis for unraveling the effects is impossible. A separation of the effect of interest could only be achieved by monitoring the signal decrease under field until saturation was reached prior to switching off the field. Apart from the disadvantage of increased measurement times, this procedure is restricted in the sub-T_G region to temperatures where physical aging does not interfere. Although a lower signal/noise ratio has to be accepted in this case, the measurement done at 60 °C (T_G − 3 K) and shown in Figure 9 indicates that the two processes can indeed be separated by this method.

Various features of other systems discussed in the literature show a strong similarity to the effects outlined above: The experimental results of Guan et al.,[23] who have observed a gradual increase of characteristic times after each poling cycle (without any thermal erase in between), can also be interpreted by our hypothesis. Goodson and Wang[26] have recently presented SHG decay data of a comparable guest/host system (PMMA/DANS) with the corresponding fits being based on a superposition of two Kohlrausch–Williams–Watts (KWW) patterns

$$M(t) = A \exp[-(t/\tau_1)^{\beta_1}] + B \exp[-(t/\tau_2)^{\beta_2}] \quad (7)$$

According to their report, the first relaxation τ_1 had been comparatively insensitive to temperature and its relative amount had decreased with increased annealing time. They concluded that a $\chi^{(3)}$ effect had been responsible for this feature. In the course of corona poling experiments with similar materials, other authors[15,27,28] have also reported about SHG signal decays with applied field. Following their discussion, residual surface charges generated by the corona discharge were considered to be responsible for this effect. In particular, Hampsch et al.[29] have specified this effect to an ion–polymer interaction set by surface charges but were not able to separate this effect. A retardation of the dopant randomization was postulated in that case, yet without further specifications. Goodson et al.[30] as well as Guan et al.[23] have also emphasized the complexity of a general explanation of these phenomena. We will refer to this point elsewhere.[31]

3. Temperature Dependence of the SHG Decay. Several series of temperature-dependent experiments were recorded within the range 50 °C ≤ T ≤ 100 °C using different samples of PIBMA/DANS. We were able to estimate the influence of dopant concentration and anode coating as well as poling voltage on the kinetics of the SHG decay. Each measurement was performed following the standardization outlined above. Hence all experiments done at a given temperature are directly comparable with respect to the sample history. Especially laser heating effects[17] are ruled out. Numerical fits to the SHG decay data were achieved following eq 8 based on a static Gaussian distribution of energy barriers with the parameters $\langle r \rangle$ and σ, which quantify the mean relaxation rate and the Gaussian width, respectively. This model, presented in detail elsewhere,[32] turned out to yield satisfactory results when applied to SHG relaxation data:[17]

$$I(t) = (2\pi\sigma^2)^{-1/2} \int_{-\infty}^{+\infty} \exp(-\epsilon^2/2\sigma^2 - \nu_0 e^{-\epsilon} t)\, d\epsilon \quad (8)$$

In a survey Figure 10 presents the temperature dependence of the mean rate $\langle r \rangle$ of the SHG decay gained from different samples, where $\langle r \rangle = \nu_0 \exp(\sigma^2/4)$ can be deduced from the slope of $I(t)$; i.e., $\langle r \rangle = -dI(t)/dt|_{t=0}$. Note that this definition of $\langle r \rangle$ via the slope applies to decay data in general; i.e., it is not model specific. Since our interest focuses on the investigation of the different fundamental factors which contribute to the dopant relaxation, the temperature dependence of the α-relaxation of pure PIBMA was determined via dielectric relaxation spectroscopy. Figure 11 compiles the mean dielectric relaxation rates (triangles) as a function of temperature as well as the SHG decay rates with field (filled squares) and the corrected SHG relaxation rates (open circles), i.e, the contribution related to the orientational randomization of chromophores.

In order to further check our SHG results, films cast from a 1% wt DANS/PIBMA solution in toluene as a solvent of different polarity (μ = 0.33 D[23]) were investigated. Choosing different drying periods the effect of solvent residues on the chromophore relaxation could be studied. The results are summarized in Table 2 and Figure 12, illustrating the effect of temperature on the mean rates of the square root of the SHG relaxation. Note that the results of the toluene samples (open triangles and squares) are readily comparable to those gained from samples cast from chloroform solution (open circles) since all measurements have been performed according to our standardization procedure.

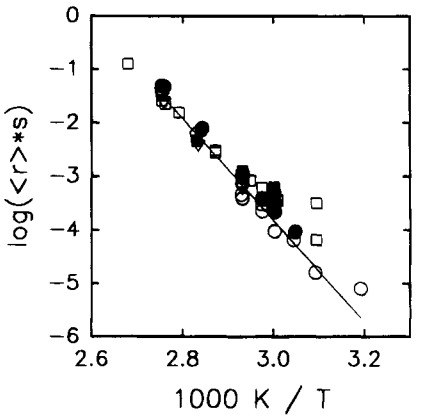

Figure 10. Arrhenius plot of the mean rate of isothermal SHG relaxation of PIBMA samples doped with DANS: open squares, uncoated anode, 0.14 MV/cm poling field, 1 wt % DANS; open triangles, SiO-coated anode, 0.14 MV/cm poling field, 0.5 wt % DANS; filled squares and circles, SiO-coated anode of different thickness, 0.14 MV/cm poling field, 1 wt % DANS; open circles, SiO-coated anode, 0.10–0.14 MV/cm poling field, 1 wt % DANS. The linear regression (solid line) refers only to data marked by open circles.

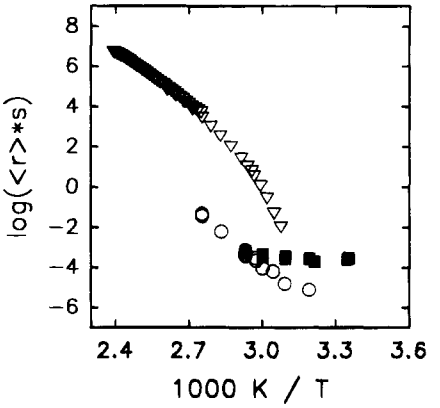

Figure 11. Survey of the temperature dependence of the α-relaxation in pure PIBMA probed by dielectric measurement (open triangles), pure orientational relaxation of 1 wt % DANS in PIBMA probed by SHG measurement (open circles), and data of the corresponding SHG relaxation with applied field (0.10 MV/cm) in this sample (filled squares).

Table 2. Activation Energies for the Data of Figure 12 as a Function of Residual Solvent

solvent	symbol	drying procedure	E_{act} (kJ/mol)
chloroform	open circle	vacuum dried at 55 °C for 2 days	181
toluene	open triangle	vacuum dried at 75 °C for 10 days	132
toluene	open square	vacuum dried at 75 °C for 6 days	114

Based on the set of experiments outlined above, the temperature dependence of the mean rate of the SHG decay in the PIBMA/DANS system was analyzed intensively. First we will refer only to those results which have been obtained by using samples cast from chloroform solutions. With respect to the data of Figure 10 the following conclusions can be drawn:

(i) Within the experimental accuracy the temperature dependence of the mean rate follows an Arrhenius behavior independent of the particular sample, the applied voltage, the coating of the anode, and the dopant content in a sample (0.5 or 1.0 wt %). The temperature

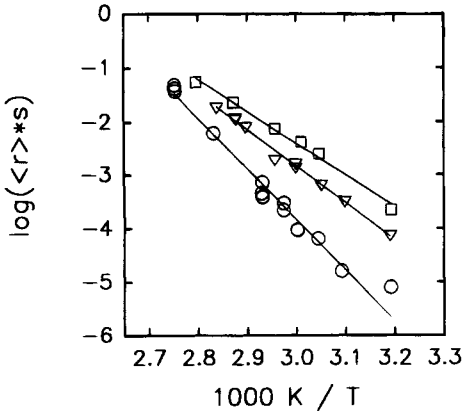

Figure 12. Arrhenius plot of the mean rate of isothermal SHG relaxation of PIBMA samples doped with 1 wt % DANS including first-order regression. The influence of using toluene (squares and triangles) instead of chloroform (circles) as a solvent for casting the films the effect of residual toluene content in the samples is presented.

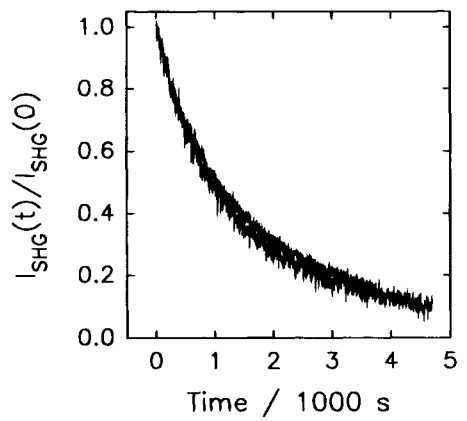

Figure 13. Representative quality of the reproducibility regarding the normalized decay data of two different PIBMA samples doped with 1 wt % DANS at T = 68 °C (T_G + 5 K). Traces have been recorded providing a constant signal level before switching off the field at t = 0.

dependence is obviously well defined, despite the poor reproducibility often claimed for the SHG technique.[33] In view of our small voltage variation, we refrain from concluding on a general independence of the decay pattern from the poling field strength.

(ii) The mean variation of relaxation rate data in Figure 10 seems to increase with decreasing temperature. However, the data which is corrected for the chloroform shielding effects (open circles) conform well with the Arrhenius line in the entire experimental range. The data scatter thus originates from the poorly reproducible shielding effect. Physical aging, expected to be active below T_G, seems not to affect the results to a significant extent. Referring only to the corrected data (open circles), an activation energy of 181 kJ/mol is determined, which is the order of magnitude expected for the apparent activation energy of the α-relaxation of PIBMA obtained from dielectric measurements by Ishida et al.[20] A detailed interpretation of these particular results will be given at the end of this section.

(iii) Separation of the signal decay with applied field simply by waiting for a constant signal level before switching off the field leads to improved reproducibility as can be seen in Figure 13 showing the traces of two different samples at T = 68 °C (T_G + 5 K).

A comparison of the SHG relaxation to the dielectric data appears in order. As a characteristic feature of polymers, the dielectric relaxation behavior of PIBMA follows the well-known WLF approach[34] or equivalently the Vogel–Fulcher–Tammann law[35]

$$\langle r\rangle = \langle r\rangle_0 e^{-B/(T-T_0)} \tag{9}$$

in agreement with previous findings.[21,36] Our SHG decay data due to orientational relaxation of the chromophore deviate significantly from the dielectric time scales since the time constants of the former process behave Arrhenius-like and are some orders of magnitude below the latter. The dielectric experiment probes the dipole–dipole correlation function of the bulk material and thus reveals the α-process which dominates the glass transition of the matrix. In contrast, the SHG method selectively probes the mean orientation of the DANS molecules. Based on the different time scales and temperature dependences of the two relaxation phenomena, one has to conclude that the chromophore orientation is strongly decoupled from the matrix motion. Possible correlations with the β-relaxation in PIBMA are not expected since this process is faster and cannot be separated from the α-relaxation in this material.[20,36] The PEMA/DANS system yielded 126 kJ/mol for the thermal activation of the reorientation of DANS and a similar offset from the dielectric relaxation as seen presently.[17] Different values are likely due to either the enhanced steric extension of the isobutyl group or the influence of different molecular weight. The interesting experiment of directly probing the DANS relaxation by dielectric relaxation spectroscopy has not been successful due to the low chromophore concentration.[21,22]

Guided by the results obtained when samples cast from toluene solutions had been used (cf. Figure 12), the temperature dependence of the SHG relaxation is confirmed once more. Small deviations being obvious for the different samples are interpreted in terms of a plasticizing effect due to residual toluene. Combined with the now strongly reduced solvent shielding effect (cf. section 2), the change in activation energy leading to an absolute acceleration of the dopant relaxation becomes plausible. In the course of tracer diffusion experiments Wang et al.[37] have also reported a significant increase of about one decade of the diffusion coefficients when adding only 0.66 wt % *p*-dichlorobenzene as a plasticizer (of similar size as toluene) to a chromophore/polycarbonate system.

The thermal course of the σ-parameter in eq 8 which quantifies the deviation from an exponential response is depicted in Figure 14, where the filled circles refer to measurements where a constant signal level prior to switching off the voltage has been guaranteed. As a rule an increase in dispersion is observed when the temperature is lowered, signifying the gradual freezing of matrix mobility. At elevated temperatures the phenomenon of "line-narrowing"[25,38] due to averaging of energy barriers partially restores exponential decay behavior. Note that σ does not increase significantly until $T \leq T_G$, especially regarding the most reliable data marked by filled circles in Figure 14. Since this feature is not paralleled by the dielectric relaxation behavior in terms of α,γ(T), this results again points toward a decoupling of the chromophore orientation from the bulk motion. All results obtained so far for PIBMA resemble the behavior of the PEMA/DANS system described previously.[17]

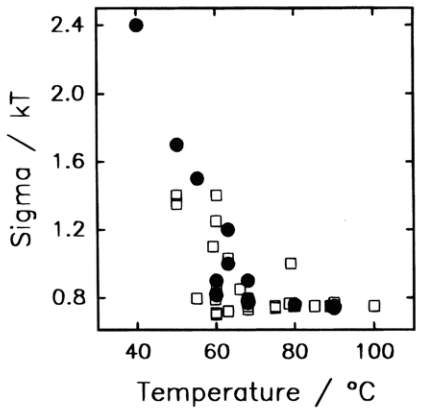

Figure 14. Variation of the dispersion parameter σ/kT with temperature for isothermal SHG relaxations for PIBMA/DANS samples. Data referring to the cases not subject to shielding effects are marked with filled circles.

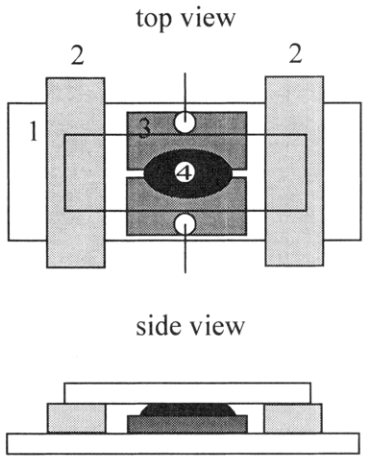

Figure 15. Design of the sample cell used for gap electrode poling of guest/host polymers: (1) borosilicate slides, (2) 25 μm Kapton sheets, (3) chrome electrodes, (4) sample film.

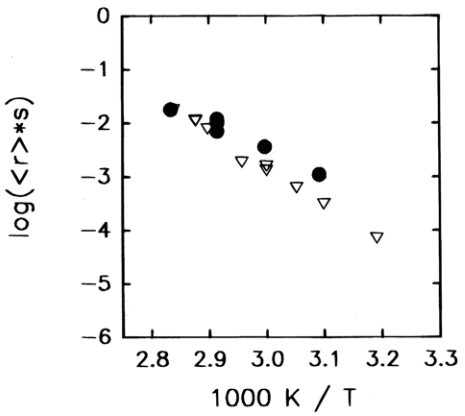

Figure 16. Arrhenius plot of the mean rate of isothermal SHG relaxation of PIBMA samples doped with 1 wt % DANS (cast from toluene solutions) using different sample cell architectures for poling: open triangles refer to ITO sandwich electrodes, closed circles refer to chrome gap electrodes.

Comparison to Literature Results

In the literature concerned with the relaxation times of SHG signals in poled polymers one finds controversy regarding the coincidence of the SHG decay time and that of the α-process. The time scales of our SHG experiments are similar to those of Goodson and Wang[26] and Guan et al.,[23] who had examined contact poled PMMA systems doped with DANS or the corresponding amino compound. On the other hand, Walsh, Stähelin, and Miller et al.[39] have presented a power law closely following the Vogel–Fulcher–Tammann approach[35,42] for the mean SHG relaxation times of various doped polymer systems. However, their study is limited to larger dopants (more than twice the size of DANS) and high chromophore concentrations of typically 15 wt %, which hampers any direct comparability to our system. Recently, Wegner et al.[43] reported about a discrepancy between SHG and dielectric decay times similar to the present results, although mainly the chromophores contribute to the dielectric response in this favorable case. Following their interpretation this behavior indicates a restricted mobility of chromophores in the stiff layered matrix of their two novel side-chain polymers. Eich et al.[15] have also compared dielectric data with SHG decay results gained from a side-chain *p*-nitroaniline polymer. Again a similar difference of the time constants was observed. In this case the authors made a surface charge decay of the corona-poled samples responsible for their results.

There is a significant disagreement between the time constants of our SHG measurements and those of Dhinojwala et al.[36] although their system merely differs by a slight increase in the molecular weight of the PIBMA with twice the dopant concentration (DANS or the corresponding azo compound). This group has reported on coincident time scales of dielectric data of the pure matrix and the SHG onset poling as well as the SHG relaxation data, implying a strong coupling of the rotational diffusion of the chromophores to the α-process of the polymer. No ambiguity arises regarding the dielectric data, since we reproduced the findings stated by Dhinojwala et al.[36] and Ishida et al.[20] Aiming at rationalizing the discrepancy of ≈5 decades in time between their data and the present results, we have determined the influence of the different sample architectures. In order to meet the conditions of a poling voltage of 2500 V applied to chrome gap electrodes with 800 μm spacing, we repeated our experiment using the 100 μm chrome gap electrode setup shown in Figure 15. In order to prevent a significant diffusion of alkali ions in the film, the electrodes were evaporated on borosilicate glass.[44] The thickness of our films was 25 μm, defined by spacer sheets instead of 5–10 μm in ref 41. The samples for our gap electrode setup were prepared in the same manner from toluene solutions as for the sandwich cells. Since only 500 V was applied across the gap to simulate the field strength of ref 41, we had to improve the focus to obtain a reasonable signal/noise ratio. Heating effects due to focusing the laser had been excluded by preliminary experiments. Due to the different geometry, the poling currents decreased by about three orders of magnitude relative to the sandwich cell case. As outlined in Figure 16 the thermal behavior of the mean relaxation rate of the samples poled via the chrome gap electrodes undoubtedly resembles the data of the sandwich poled samples. The effect of different field strengths can be estimated not to exceed 0.5 decade[31] in this system. In conclusion, a different sample setup obviously does not cause the discrepancy of the results mentioned above. A further problem in comparing our data to that of ref 41 stems from the lack of information regarding their sample history prior to each measurement. According to our experience and to work of Guan et al.,[23] both the SHG relaxation and poling time scale are affected considerably when a thermal erase process is insufficient or omitted.

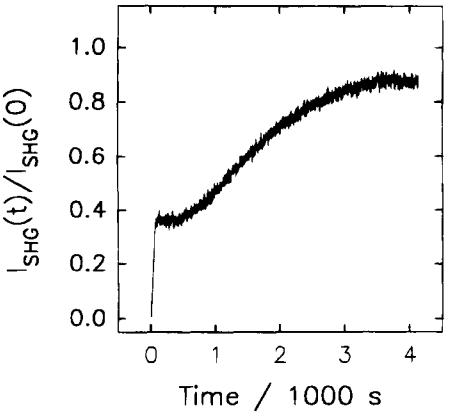

Figure 17. Demonstration of a fast switching effect, an apparent steady-state value, and a subsequent slow increase in the SHG efficiency in the course of poling a PIBMA sample doped with 1 wt % DANS (T = 90 °C, E = 0.14 MV/cm).

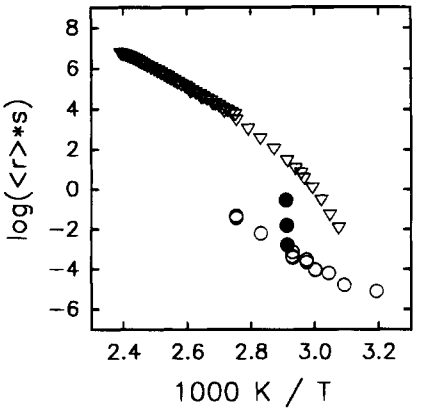

Figure 18. Demonstration of the impact of laser focusing on the results of SHG relaxation measurements. Filled circles refer to the mean relaxation rate of 1 wt % DANS in PIBMA at T = 70 °C for various laser spot sizes. Open triangles and circles refer to the dielectric and standard SHG measurements as in Figure 11.

Despite the difference of the film thickness by (only) a factor 2−3 of our measurements and those of ref 41, we exclude different amounts of residual solvent being responsible for the discrepancy of 5 decades in kinetics due to the following: (i) Compared to our samples those used in ref 41 had been dried quite weakly (24 h below T_G, 12 h above T_G under vacuum without controlling the solvent removal). We have simulated this drying procedure using a 1 wt % DANS/PIBMA film of 7 ± 2 μm thickness and solvent cast from a chloroform solution. Vacuum drying at T = 45 °C for 24 h yielded 0.8% of chlorine residues. Further backing of the very same film for 15 h at T = 70 °C in vacuum resulted in 0.54% residual chlorine. Obviously our films (~0.8% chlorine; cf. section 2) as well as the films used in ref 41 contain similar amounts of residual solvent. (ii) A higher solvent content in our samples should cause an accelerated dopant relaxation due to plasticizer effects while our experiments show the opposite. (iii) The basic discrepancy remains unaffected by the various different experimental conditions covered in the present study, e.g., chloroform versus toluene solvent.

In the course of poling experiments, in particular with samples cast from chloroform solutions, switching effects have been observed occasionally, which could not be time resolved by a 10 Hz sampling rate. In such cases an almost instantaneous rise of the SHG signal followed by a constant level for times up to a few minutes was observed, which suggests a very rapid and complete poling process. This feature depends on the experimental conditions and is more pronounced at lower temperature and at lower poling fields. Continuous monitoring of the poling process indicates that the apparent steady-state SHG signal increases further to eventually attain much higher values as shown in Figure 17. The onset-poling technique presented in ref 41 is likely to detect only the fast process. Moreover, we do not confirm their assumption of full reversibility of both poling and relaxation processes without an erase step on the time scale of milliseconds which has been substantial for their data sampling process in the short-time domain. The origin of these fast switching effects is presently not well understood and still a matter of speculation.

As a final point of experimental uncertainty, we wish to emphasize that heating effects caused by the intense 1064 nm laser beam can have a strong impact on the SHG decay. An impressive example for this is depicted in Figure 18, where the effect of varying the focus at a given sample temperature (T = 70 °C) is presented in the context of results from dielectric and SHG experiments (see also Figure 11). By successive focusing an acceleration of about three orders of magnitude in the relaxation rate was achieved, which corresponds to a shift in the effective temperature by about 30 K, although our chopper system strongly attenuates the incident beam.

Summary and Conclusion

Employing the SHG technique, the dynamics of orientational relaxation of DANS in PIBMA has been investigated within a temperature range of 50 K encompassing T_G. Solvent-cast films were electrode poled in a transparent ITO-coated sandwich cell. Although the charge-carrier density monitored by the cell current was varied by more than one order of magnitude by SiO-coated anodes, no significant impact on the relaxation kinetics was detected. We have studied in detail the contribution to the SHG relaxation which proceeds irrespective of the absence of the poling voltage, which therefore should not be related to the orientational randomization of chromophores. Based on its low activation energy (15 kJ/mol) and solvent dependence (chloroform versus toluene), we tentatively ascribe this feature to a shielding effect of dipolar (solvent) impurities. Consequently, changes of the local field factors and the molecular hyperpolarizability rather than orientational relaxation of the chromophores are assumed to influence the SHG intensity in this field-independent case. Separating the decay under field from the decay which is induced by removing the external field leads to more reliable and reproducible SHG decay data for the process which does involve the orientational dynamics of the dopant molecules. Especially at lower temperatures a satisfactory reproducibility is achieved only if steady-state conditions are reached prior to switching off the field.

Evaluation of the corrected SHG decay data corresponding to orientational relaxation has been done assuming a static Gaussian distribution of activation energies for orientational motion, which gave superior fits compared to the KWW function. The mean SHG rates were found to follow an Arrhenius law whereas the α-process of PIBMA inferred from dielectric measurements is better represented by a VFT function. Additionally, the absolute rates of these two processes

differ by several orders of magnitude. This pronounced decoupling of the SHG relaxation from the α-process remains unaffected by separating the shielding effect. Minor differences in the temperature dependences when changing the solvent from chloroform to toluene were interpreted in terms of plasticizing effects. At present, we cannot present a reasonable explanation for the slow and Arrhenius-like behavior of SHG time scales. Further work concerning experiments which might help to clarify the difference between the time scales of dielectric and SHG measurements is in progress.

Acknowledgment. We gratefully acknowledge the support of the Philipps-Universität Marburg in terms of a Ph.D. scholarship. We thank Prof. E. O. Göbel for providing the Nd-YAG laser, Prof. V. Arkhipov for very helpful discussions concerning the model of mesoscopic shielding, J. Schüller for the support concerning the dielectric measurements, and Dr. H. Mell for the help in preparing the chrome gap electrodes.

References and Notes

(1) Havinga, E. E.; Van Pelt, P. *Ber. Bunsenges. Phys. Chem.* **1979**, *83*, 816.
(2) Meredith, G. R.; Van Dusen, J. G.; Williams, D. J. *Macromolecules* **1982**, *15*, 1385.
(3) Pantelis, P.; Hill, J. R.; Oliver, S. N.; Davies, G. J. *Br. Telecom Technol. J.* **1988**, *6*, 3.
(4) Prasad, P. N.; Williams, D. J. *Introduction to Nonlinear Optical Effects in Molecules and Polymers*; Wiley-Interscience: New York, 1991.
(5) Staring, E. G. J. *Recl. Trav. Chim. Pays-Bas* **1991**, *110*, 492.
(6) Buckley, A. *Adv. Mater.* **1992**, *4*, 153.
(7) Willand, C. S.; Williams, D. J. *Ber. Bunsenges. Phys. Chem.* **1987**, *91*, 1304.
(8) Ulrich, D. R. *Mol. Cryst. Liq. Cryst.* **1988**, *160*, 1.
(9) Eich, M.; Bjorklund, G. C.; Yoon, D. Y. *Polym. Adv. Technol.* **1990**, *1*, 189.
(10) Ediger, M. D. *Annu. Rev. Phys. Chem.* **1991**, *42*, 225.
(11) Hyde, P. D.; Evert, T. E.; Ediger, M. D. *J. Chem. Phys.* **1990**, *93*, 2274.
(12) Hyde, P. D.; Ediger, M. D.; Kitano, T.; Ito, K. *Macromolecules* **1989**, *22*, 2253.
(13) Ehlich, D.; Sillescu, H. *Macromolecules* **1990**, *23*, 1600.
(14) Köhler, W.; Robello, D. R.; Willand, C. S.; Williams, D. J. *Macromolecules* **1991**, *24*, 4589.
(15) Eich, M.; Sen, A.; Looser, H.; Bjorklund, G. C.; Swalen, J. D.; Twieg, R.; Yoon, D. Y. *J. Appl. Phys.* **1989**, *66*, 2559.
(16) Köhler, W.; Robello, D. R.; Dao, P. T.; Willand, C. S.; Williams, D. J. *J. Chem. Phys.* **1990**, *93*, 9157.
(17) Schüssler, S.; Richert, R.; Bässler, H. *Macromolecules* **1994**, *27*, 4318.
(18) Chemla, D. S.; Zyss, J., Eds. *Nonlinear Optical Properties of Organic Molecules and Crystals*; Academic Press: New York, 1987.
(19) Arkhipov, V., private communication.
(20) Ishida, Y.; Yamafuji, K. *Kolloid Zeit.* **1961**, *177*, 97.
(21) Glüsen, B. Thesis, Philipps-Universität Marburg, Germany, 1993.
(22) Baehr, C.; Glüsen, B.; Wendorff, J. H.; Staring, E. G. J. *Macromol. Rapid. Commun.* **1994**, *15*, 327.
(23) Guan, H. W.; Wang, C. H.; Gu, S. H. *J. Chem. Phys.* **1994**, *100*, 8454.
(24) Weast, R. C., Ed. *Handbook of Chemistry and Physics*; CRC Press: Cleveland, 1978.
(25) Albrecht, U.; Schäfer, H.; Richert, R. *Chem. Phys.* **1994**, *182*, 61.
(26) Goodson, T.; Wang, C. H. *Macromolecules* **1993**, *26*, 1837.
(27) Hampsch, H. L.; Yang, J.; Wong, G. K.; Torkelson, J. M. *Macromolecules* **1990**, *23*, 3648.
(28) Mortazavi, M. A.; Knoesen, A.; Kowel, S. T.; Higgins, B. G.; Dienes, A. *J. Opt. Soc. Am. B* **1989**, *6*, 733.
(29) Hampsch, H. L.; Torkelson, J. M.; Bethke, S. J.; Grubb, S. G. *J. Appl. Phys.* **1990**, *67*, 1037.
(30) Goodson, T., III; Gong, S. S.; Wang, C. H. *Macromolecules* **1994**, *27*, 4278.
(31) Schüssler, S.; Richert, R.; Bässler, H., to be published.
(32) Richert, R. In *Optical Techniques to Characterize Polymer Systems*; Bässler, H., Ed.; Elsevier: Amsterdam, The Netherlands, 1989.
(33) Hampsch, H. L.; Yang, J.; Wong, G. K.; Torkelson, J. M. *Polym. Commun.* **1989**, *30*, 40.
(34) Williams, M. L.; Landel, R. F.; Ferry, J. D. *J. Am. Chem. Soc.* **1955**, *77*, 3701.
(35) Vogel, H. *Phys. Z.* **1921**, *22*, 645; Fulcher, G. S. *J. Am. Ceram. Soc.* **1923**, *8*, 339.
(36) Dhinojwala, A.; Wong, G. K.; Torkelson, J. M. *Macromolecules* **1993**, *26*, 5943.
(37) Wang, C. H.; Xia, J. L.; Yu, L. *Macromolecules* **1991**, *24*, 3638.
(38) Richert, R. *Chem. Phys.* **1988**, *122*, 455; *Mol. Cryst. Liq. Cryst.* **1990**, *183*, 283.
(39) Stähelin, M.; Burland, D. M.; Ebert, M.; Miller, R. D.; Smith, A.; Twieg, A.; Volksen, W.; Walsh, C. A. *Appl. Phys. Lett.* **1992**, *61*, 1626.
(40) Walsh, C. A.; Burland, D. M.; Lee, V. Y.; Miller, R. D.; Smith, B. A.; Twieg, R. J.; Volksen, W. *Macromolecules* **1993**, *26*, 3720.
(41) Miller, R. D.; Burland, D. M.; Lee, V.; Moylen, C. M.; Staehelin, M.; Twieg, R. J.; Volksen, W.; Walsh, C. A. Conference on Polymers for Microelectronics, Kawasaki, Japan, 1993, p 257.
(42) Aklonis, J.; MacKnight, W. *Introduction to Polymer Viscoelasticity*; Wiley-Interscience: New York, 1983.
(43) Wegner, G.; Neher, D.; Heldmann, C.; Servay, T. K.; Winkelmann, H. J.; Schulze, M.; Kang, C. S. *Mater. Res. Soc. Symp. Proc.* **1994**, *328*, 15.
(44) Mell, H., private communication.

MA9450750